Physiologia Plantarum
An International Journal for Plant Biology

Physiologia Plantarum 154: 358–368. 2015

The effect of atmospheric carbon dioxide concentrations on the performance of the mangrove *Avicennia germinans* over a range of salinities

Ruth Reef[a,*], Klaus Winter[b], Jorge Morales[b], Maria Fernanda Adame[c], Dana L. Reef[a] and Catherine E. Lovelock[a]

[a]School of Biological Sciences, The University of Queensland, St Lucia 4072, Australia
[b]Smithsonian Tropical Research Institute, Panama 0843-03092, Republic of Panama
[c]Australian Rivers Institute, Griffith University, Nathan 4111, Australia

Correspondence
*Corresponding author,
e-mail: r.reef@uq.edu.au

Received 12 May 2014;
revised 13 August 2014

doi:10.1111/ppl.12289

By increasing water use efficiency and carbon assimilation, increasing atmospheric CO_2 concentrations could potentially improve plant productivity and growth at high salinities. To assess the effect of elevated CO_2 on the salinity response of a woody halophyte, we grew seedlings of the mangrove *Avicennia germinans* under a combination of five salinity treatments [from 5 to 65 parts per thousand (ppt)] and three CO_2 concentrations (280, 400 and 800 ppm). We measured survivorship, growth rate, photosynthetic gas exchange, root architecture and foliar nutrient and ion concentrations. The salinity optima for growth shifted higher with increasing concentrations of CO_2, from 0 ppt at 280 ppm to 35 ppt at 800 ppm. At optimal salinity conditions, carbon assimilation rates were significantly higher under elevated CO_2 concentrations. However, at salinities above the salinity optima, salinity had an expected negative effect on mangrove growth and carbon assimilation, which was not alleviated by elevated CO_2, despite a significant improvement in photosynthetic water use efficiency. This is likely due to non-stomatal limitations to growth at high salinities, as indicated by our measurements of foliar ion concentrations that show a displacement of K^+ by Na^+ at elevated salinities that is not affected by CO_2. The observed shift in the optimal salinity for growth with increasing CO_2 concentrations changes the fundamental niche of this species and could have significant effects on future mangrove distribution patterns and interspecific interactions.

Introduction

The persistent rise in atmospheric CO_2 concentrations over the last two centuries from a preindustrial level of approximately 280 ppm to currently about 400 ppm is having a pronounced effect on the physiology of most plant species. An increase in CO_2 concentrations generally stimulates photosynthesis and growth (Ainsworth and Long 2005) and increases plant water-use efficiency (Drake et al. 1997). For salt tolerant plants the effects of elevated CO_2 on growth and photosynthesis are unclear.

Salinity represents a physiological challenge for plants because water acquisition is more difficult and because ions (mainly Na^+ and Cl^-), although required for osmotic adjustment and turgor maintenance, can accumulate in the tissues to toxic concentrations (Scholander et al. 1962). Both of these stressors can lead to oxidative stress and lower rates of photosynthesis and growth (Ball

Abbreviations – CI, confidence interval; HSD, honest significant difference; ppt, parts per thousand; RUBISCO, ribulose-1,5-bisphosphate carboxylase/oxygenase; SL, stem length; SLA, specific leaf area; SRL, specific root length.

1988). If growth rate under saline conditions is inhibited by the rate of supply of photosynthates, elevated atmospheric CO_2 concentrations could have a positive effect on growth rates by increasing intracellular CO_2 concentrations under saline conditions while maintaining high water use efficiency (Geissler et al. 2009).

Mangroves are trees that grow in saline, tidal wetlands on tropical and subtropical coastlines and can tolerate a wide range of soil salinity (Lugo and Snedaker 1974, Odum et al. 1982, Hutchings and Saenger 1987). Nonetheless, salinity has long been recognized as an important factor that limits mangrove growth (Lin and Sternberg 1992, Ball 2002, Lovelock et al. 2006) and is an important environmental variable in determining mangrove species distribution and interspecific interactions (Bunt et al. 1982, Ball 1988, Smith 1988, Ball 1998). Thus, changes to the response of plants to salinity with increasing CO_2 could have significant ecological consequences.

Even in plants that are not salt tolerant the responses to elevated CO_2 can be complex. The CO_2 response of some plants has been shown to depend on other environmental variables that can potentially limit growth (such as nutrient availability). Many long-term experiments have shown an 'acclimation' of photosynthesis to higher CO_2 levels (Drake et al. 1997), which is caused by the downregulation of photosynthesis genes and ribulose-1,5-bisphosphate carboxylase/oxygenase (RUBISCO) activity. Decreased RUBISCO activity is brought about, in part, by an accumulation of starch in the leaves and a range of other molecular and biochemical feedbacks (Pritchard et al. 1997, Stitt and Krapp 1999). This acclimation is observed mainly in plants where growth is limited by non-stomatal factors, such as nutrient limitation (Ainsworth et al. 2004). In those plants, elevated CO_2 does not sustain the expected higher levels of photosynthesis or growth. Salinity inhibits plant growth through both stomatal and non-stomatal processes; thus, despite the benefit from potentially increased intracellular CO_2 concentrations and water use efficiency, mangrove growth and photosynthesis might not be stimulated by elevated CO_2.

The aims of this study were to measure the effects of atmospheric CO_2 concentrations under a range of salinity conditions in the common and widespread mangrove *Avicennia germinans* to determine how rising CO_2 levels might affect *A. germinans* growth, root traits, photosynthesis, ion relations, water use and salt accumulation and whether productivity and growth reduction due to salt stress is ameliorated as CO_2 concentrations increase. This was achieved by growing *A. germinans* seedlings at three CO_2 concentrations (280, 400 and 800 ppm) over five levels of root zone salinity.

Materials and methods

Mangrove collection and propagation

Mature propagules of *A. germinans* (n = 200) were collected on August 7, 2012 and August 8, 2012 at Galeta Point, Panama (9°24′01″N, 79°51′51″W). The mangrove forest at this site is comprised of *A. germinans*, *Laguncularia racemosa*, *Rhizophora mangle* and *Conocarpus erectus* (Reef personal observation). The pore water salinity within *A. germinans* dominated areas of the forest at the time of propagules collection ranged from 11 to 43 parts per thousand (ppt) with a mean ± SD of 25.5 ± 12.5 ppt. Rainfall in the region is approximately 2750 mm $year^{-1}$ (Galeta Point Physical Monitoring Programme) which falls mainly in the rainy season (April to December). Propagules were collected during the rainy season. The propagules were placed in seedling trays filled with local mangrove soil. The seedlings trays were placed 0.5 m above the ground and covered with netting to prevent herbivory by crabs and insects. The mangroves were grown in open air, shaded conditions and were watered daily with a 1:10 (v:v) sea water:tap water solution. On September 10, 2012, 150 similar sized seedlings were transplanted to Santa Cruz Experimental Field Facility, Smithsonian Tropical Research Institute, Gamboa, Panama (9°07′N, 79°42′W) and planted in individual 1.6 l tree pots (7 × 10 × 23 cm) filled with a mixture (50%/50%) of local topsoil and sand. Seedling height averaged 13 cm at the time and most seedlings had two leaf pairs and had lost their cotyledons (i.e. exhausted their maternal carbon reserves).

Experimental conditions

Plants were divided among three glasshouses (n = 50 pots per glasshouse), first had CO_2 concentrations similar to ambient (400 ppm), second had CO_2 concentrations similar to preindustrial CO_2 levels (280 ppm) and the third had an elevated CO_2 concentration of 800 ppm (the IPCC A2 scenario for the end of the century). Elevated CO_2 was maintained by releasing CO_2 gas from a high-pressure cylinder in brief pulses when the CO_2 concentration in the glasshouse fell to 790 ppm. Injection of CO_2 stopped when the CO_2 concentrations reached 810 ppm. Preindustrial [CO_2] was maintained between 270 and 290 ppm by scrubbing CO_2 from the air using a column of soda lime, and air pump and dust bag of an industrial vacuum cleaner. The glasshouses were equipped with split air conditioning units programmed to turn on when the air temperature exceeded 30°C. Air temperature and relative humidity were recorded in the three glasshouses every 15 min with a data logger (CR10X; Campbell Scientific, Logan,

Table 1. Measurements of the atmospheric conditions in the three glasshouses between September 11, 2012 and February 2, 2013.

Parameter measured	280 ppm, glasshouse	400 ppm, glasshouse	800 ppm, glasshouse
Mean air temperature (°C) ± SD	28.2 ± 0.9	28.5 ± 1.3	27.8 ± 1.1
Mean relative humidity (%) ± SD	67.4 ± 13.2	66.7 ± 16.4	65.4 ± 18.1
Mean [CO_2] (ppm) ± SD	284.8 ± 32.8	405.7 ± 14.0	808.6 ± 46.7

UT). The atmospheric conditions in each of the three glasshouses are summarized in Table 1.

Seedlings were watered twice weekly with 300 ml salt solution that saturated the pots. The soil remained moist, but not saturated, between watering treatments. Five salinity treatments were implemented in each glasshouse using 5, 20, 35, 50 or 65 g l^{-1} of instant ocean aquarium salt (n = 10 plants for each salinity level in each glasshouse). Salinity treatments were chosen to cover the range of salinities in which this species naturally occurs (Goncalves-Alvim et al. 2001). Instant ocean aquarium salt does not contain nitrogen and phosphorus and nutrients were added weekly to all watering solutions at a concentration of 0.06 m*M* KNO_3, 0.04 m*M* $Ca(NO_3)_2$, 0.01 m*M* $NH_4H_2PO_4$, 0.01 m*M* $(NH_4)_2HPO_4$, 2.5 µ*M* H_3BO_3, 0.2 µ*M* $MnSO_4$, 0.2 µ*M* $ZnSO_4$, 0.05 µ*M* $CuSO_4$, 0.05 µ*M* H_2MoO_4, 2 µ*M* $C_{10}H_{12}FeN_2NaO_8$ [ethylenediaminetetraacetic acid iron (III)-sodium salt]. Once a week the plants received a shower of fresh water (10 ml) from a spray bottle to simulate a rain event washing the salt from their leaves.

Acclimation procedures

On September 11, seedlings were randomly distributed among 15 salinity × CO_2 treatments (n = 10 for each treatment). Soil salinity was increased gradually in steps of 5 ppt to avoid shock. The highest salt concentration of 65 ppt was achieved on December 6, 2012. From this point, plants were irrigated twice weekly with the final salinity treatment (5, 20, 35, 50 and 65 ppt), until the harvest from January 30, 2013 to February 2, 2013. The experimental period was short in order to avoid restrictions to root growth in the pots, which has been demonstrated to influence responses to elevated CO_2 in other studies (Thomas and Strain 1991).

Stem elongation, biomass, leaf area, root morphology and elemental composition

Seedling height, number of nodes and number of leaves were measured for all seedlings when they were allocated to the different CO_2 or salinity treatments in September. The same measurements were made when final treatment salinity concentrations were reached (December) and again immediately before the harvest (February). Following the harvest, plants were split into above and below ground components. Leaf area was measured using a LI-3100C leaf area meter (Li-Cor Corp., Lincoln, NE). Roots were photographed and analyzed using WINRHIZO root analysis software (Regent Instruments Inc., Quebec, QC, Canada). Plant material was then washed in distilled water to remove external salt and dried at 70°C for 5 days and weighed.

Root images of each seedling were analyzed using WINRHIZO 2007b (Regent Instruments Inc.) for total root length, average root diameter, root volume and surface area. Specific root length (SRL) was then calculated as the product of root length divided by root biomass. Root tissue density was calculated as the product of root biomass divided by root volume.

Samples for nutrient leaf concentrations and isotopic composition were taken from the same leaves used for photosynthesis measurements from five randomly selected plants from each treatment. The isotopic composition of the added CO_2 in the 800 ppm treatment differed slightly from that in ambient air. The correction for this was previously determined for this system by growing two C4 plants (*Saccharum spontaneum* and *Portulaca oleracea*) in the chambers. A correction factor of 2‰ was subtracted from the foliar $\delta^{13}C$ values of seedlings from the 800 ppm treatment (Cernusak et al. 2011).

Leaves were washed with distilled water and dried at 70°C for a week and ground prior to analysis. Leaf carbon (C) and N concentrations and their stable isotope abundances were analyzed at the Smithsonian Tropical Research Institute Biogeochemistry Lab using a Flash HT Elemental Analyzer coupled through a Conflo III interface to a Delta V Advantage continuous flow isotope ratio mass spectrometer (Thermo Scientific, Bremen, Germany). Phosphorus, calcium, magnesium, potassium and sodium in leaves were determined by digestion under pressure in concentrated HNO_3 with detection by inductively coupled plasma optical-emission spectrometry (Optima 7300 DV; Perkin Elmer Inc., Shelton, CT).

Statistical analyses were performed using R version 3.0.2 with packages MASS and sm. Where the response of seedling growth to salinity and CO_2 was unimodal, data were fit to a Gaussian model and distribution parameters (such as center of distribution and amplitude) were used to define the growth response

to salinity. Significant differences in these parameters between CO_2 treatments were tested using a two sample Kolmogorov–Smirnov test.

Gas exchange measurements

Net photosynthetic CO_2 assimilation rate (A) and stomatal conductance to water vapor (Gs) were measured with a Li-Cor 6400 portable photosynthesis system (Li-Cor Corp.) equipped with a 6400-60 leaf chamber. The measurements were made on the youngest fully expanded leaves between 09:00 and 11:30 h the day following the irrigation with nutrient solution (n ranged from 6 to 10 per treatment depending on the number of live seedlings). This was repeated for 4 weeks and all statistical analyses were performed on the average value of each seedling over the 4 weeks of measurement.

The CO_2 concentration in the cuvette was set at 280 ppm (for preindustrial plants), 400 ppm (for ambient CO_2 plants) and 800 ppm (for future CO_2 plants) using a CO_2 injector (6400-01) and compressed CO_2 cartridges (Li-Cor Corp.). Leaf temperature, measured using an infrared thermometer (Raytek Corp. Santa Cruz, CA) averaged 32°C during the measurement period (n = 50), so leaf temperature within the cuvette was set to 32°C. When leaves did not completely cover the cuvette window, one-sided (projected) leaf areas within the cuvette were measured and gas exchange data recomputed using the LI-6400 simulator software (ver. 5, Li-Cor Corp.).

Initial light-response curves (Fig. S1, Supporting Information), indicated light saturated photosynthesis at irradiance values <1000 µmol quanta m^{-2} s^{-1}; thus 1000 µmol quanta m^{-2} s^{-1} was chosen as the saturation light level for light saturated net CO_2 uptake measurements. Light in the cuvette was provided by a red LED source (6400-02, Li-Cor Corp.).

Statistical tests of the effects of the treatments on leaf gas exchange parameters were based on an ANCOVA using the lm function in R with salinity as a covariate and CO_2 as a factor.

Results

Stem elongation and survivorship

Increments in stem length (SL, cm) over the final salinity treatment period (52 days) were used as the proxy for growth. Final SL was significantly and positively correlated with both the final above ground biomass: AGB (g) = 0.12 × SL − 0.46, $R^2 = 0.69$, $P < 0.001$; and final total biomass: TB (g) = 0.19 × SL − 0.49, $R^2 = 0.66$, $P < 0.001$. Final SL was also significantly and positively correlated with final leaf number (Fig. S2), indicating no significant change in biomass allocation patterns to leaves and stems among the CO_2 treatments ($F_{(2,124)} = 2$, $P = 0.14$).

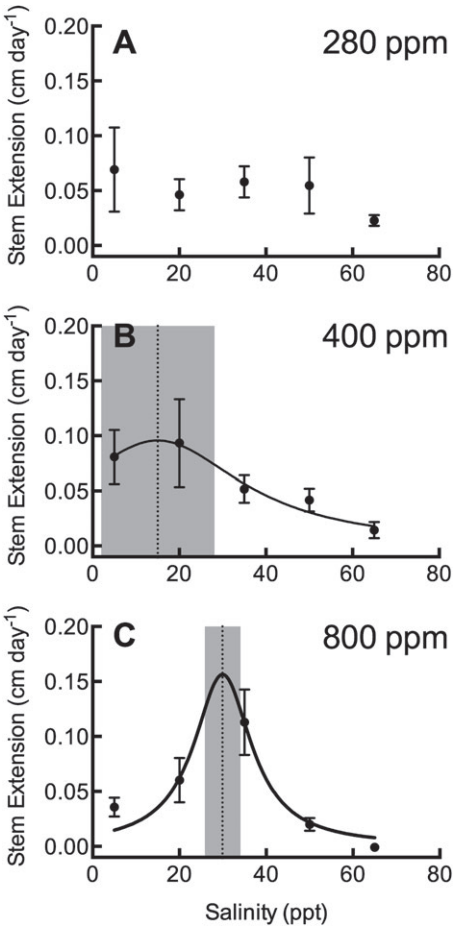

Fig. 1. Mean (±SE, n = 6–10) stem extension rates (cm day^{-1}) as a function of salinity for seedlings grown under three different atmospheric CO_2 concentrations: (A) 280 ppm (B) 400 ppm and (C) 800 ppm. Gaussian models were fitted to the data for the 400 and 800 ppm CO_2 treatments ($R^2 = 0.17$ and 0.44 for 400 and 800 ppm, respectively), dotted lines represent the mean center of the distribution and shaded areas are the 95% confidence intervals around the mean.

Stem extension rate (cm day^{-1}) revealed a significant shift in salinity optima for growth in response to changes in glasshouse CO_2 concentrations (Fig. 1). At 280 ppm, growth rates were not significantly affected by salinity level ($P = 0.22$, Fig. 1A) but were highest at the lowest salinity level. At higher CO_2 concentrations the response of seedling growth to salinity and CO_2 became unimodal (Fig. 1B, C) thus data were fit to Gaussian models and distribution parameters (e.g. the center of the distribution and its amplitude) were used to define the growth response to salinity. Growth rates of seedlings at 400 ppm were described by the model

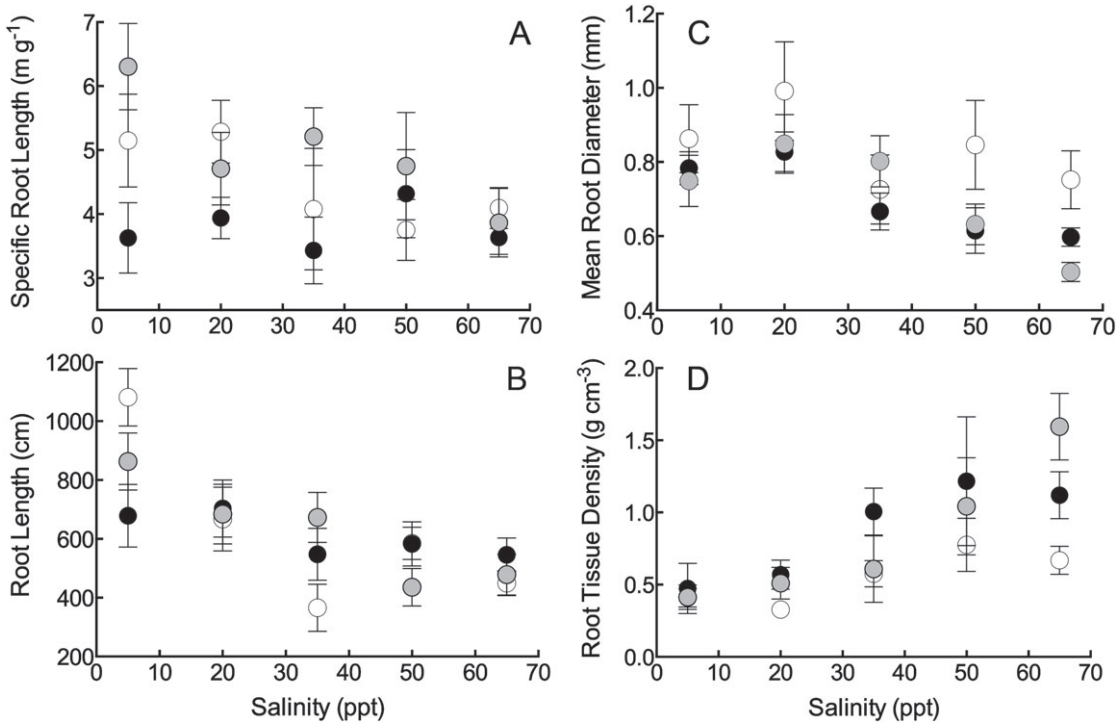

Fig. 2. Root architecture as a function of soil salinity for seedlings grown under three different atmospheric CO_2 concentrations: 280 ppm (open circles), 400 ppm (gray shaded circles) and 800 ppm (filled circles). (A) Mean SRL m g^{-1}. (B) Mean root length (cm). (C) Mean root diameter (mm) and (D) Root tissue density (g cm^{-3}). Values are the average (±SE) of 7–10 seedlings per treatment.

$SL = 0.1/(1 + ((salinity - 15)/24)^2)$, $R^2 = 0.17$. Optimal growth rates at 400 ppm CO_2 were achieved at salinities of 15 ± 6.5 ppt 95% confidence interval (CI; Fig. 1B). At 800 ppm optima for growth shifted to even higher salinities (29.9 ± 2.03 ppt 95% CI; Fig. 1C). At 800 ppm, the model fitted was $SL = 0.16/(1 + ((salinity - 29.9)/8)^2)$ with an R^2 of 0.44. The growth optima (the salinity where maximal growth rates were achieved) shifted to significantly higher salinities as CO_2 partial pressure increased (comparison of fit of the Gaussian models to a global fitted model $F_{(2,119)} = 4.6$, $P = 0.01$). While the center of the distribution significantly shifted to higher salinities as CO_2 concentrations increased, the maximum growth rates achieved at the salinity optima (the amplitude of the distribution) were not significantly different between the CO_2 treatments ($F_{(2,119)} = 0.59$, $P = 0.56$).

Mortality rates of seedlings were relatively low (11%). In the majority of the treatments (8/15) all 10 seedlings survived. Mortality rates were significantly higher in the 800 ppm CO_2/5 ppt salinity treatment, where only 4 of 10 seedlings survived (Chi-square = 28.4, d.f. = 8, $P < 0.001$). Mortality rates in the other treatments where mortality occurred ranged from 10% (three treatments) and 20% (800 ppm CO_2/50 ppt) to 30% (two treatments, 400 ppm CO_2/50 ppt and 800 ppm CO_2/35 ppt).

Both salinity and CO_2 had a significant effect on root architecture. SRL was lower in the high CO_2 treatment [ANCOVA, $F_{(2,123)} = 4$, $P = 0.02$, Tukey honest significant difference (HSD) 800–400 ppm $P = 0.01$; Fig. 2A]. Salinity also had a significant negative effect on SRL ($F_{(1,123)} = 8.5$, $P = 0.004$). Root length decreased significantly with salinity ($F_{(1,125)} = 30.8$, $P < 0.001$, Fig. 2B) but was not affected by CO_2 ($P = 0.96$). Mean root diameter was smaller as salinity increased (ANCOVA, $F_{(1,121)} = 16.3$, $P < 0.001$, Fig. 2C) and also as CO_2 increased (ANCOVA, $F_{(2,121)} = 4.7$, $P = 0.01$). Plants grown under CO_2 concentrations of 280 ppm had significantly thicker roots than those grown at 400 or 800 ppm (Tukey HSD, $P = 0.02$ and $P = 0.03$, respectively). Root tissue density was also affected by both CO_2 and salinity. Plants grown under CO_2 concentrations of 280 ppm had significantly lower root tissue density than plants grown under higher concentrations ($F_{(2,121)} = 4.6$, $P = 0.01$; Fig. 2D). Tissue density increased with increasing salinities ($F_{(1,121)} = 34.7$, $P < 0.001$) especially in the higher CO_2 treatments (interaction $P = 0.05$). Root/shoot ratios were not significantly affected by CO_2 concentrations or by salinity and were on average 0.73 (±0.2 SD).

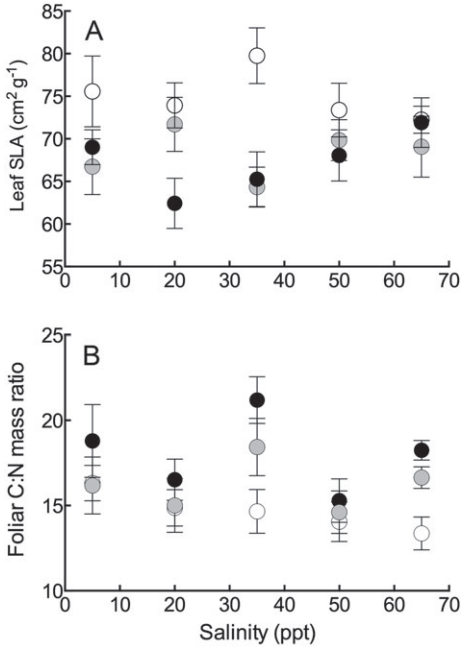

Fig. 3. Foliar properties as a function of soil salinity for seedlings grown under three different atmospheric CO_2 concentrations: 280 ppm (open circles), 400 ppm (gray shaded circles) and 800 ppm (filled circles). (A) SLA cm^2 g^{-1}. (B) Foliar C:N mass ratio. Values are the average (±SE) of four to five seedlings per treatment.

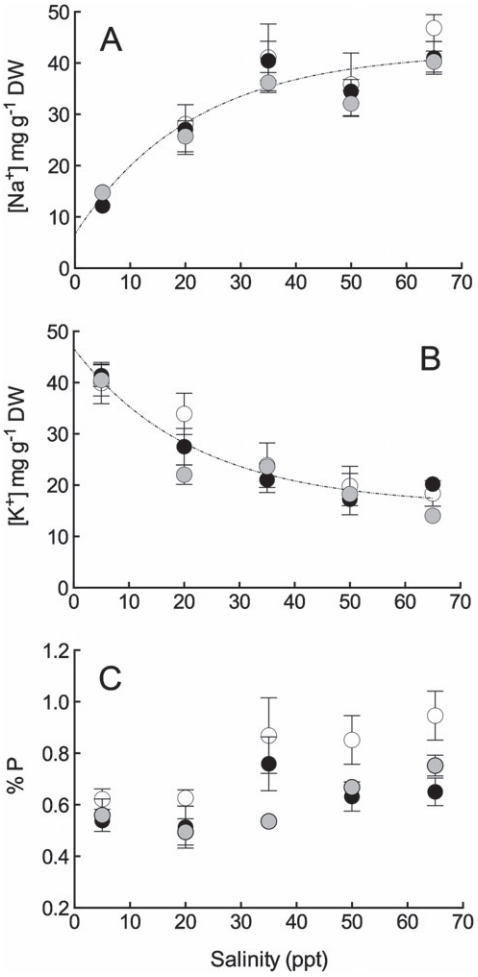

Fig. 4. Foliar ion and phosphorus concentrations as a function of soil salinity for seedlings grown under three different atmospheric CO_2 concentrations: 280 ppm (open circles), 400 ppm (gray shaded circles) and 800 ppm (filled circles). (A) Na^+ (mg g^{-1} dry weight) (B) K^+ (mg g^{-1} dry weight) and (C) P (mg 100 mg^{-1} dry weight). Values are the average (±SE) of four to five seedlings per treatment. (A) and (B) fitted with exponential curves (one curve shown combining the three CO_2 concentrations, $R^2 = 0.59$ and 0.6 for (A) and (B), respectively).

Leaf properties

Specific leaf area (leaf biomass per unit area, SLA; Fig. 3A) was significantly higher in plants grown under preindustrial CO_2 concentrations compared with plants grown under ambient and predicted future CO_2 concentrations (ANCOVA, $F_{(2,119)} = 9.6$, $P < 0.001$ and Tukey HSD; Fig. 3A). A lower leaf C:N ratio was also measured in plants grown under preindustrial CO_2 concentrations (ANCOVA, $F_{(2,67)} = 7.4$, $P = 0.001$; Fig. 3B). Salinity had no effect on SLA ($F_{(1,119)} = 0.24$, $P = 0.63$) or on foliar C:N ratios ($F_{(1,67)} = 1$, $P = 0.32$).

Foliar Na^+ concentrations were not affected by CO_2 ($F_{(6,66)} = 0.55$, $P = 0.8$). Foliar Na^+ concentrations increased with salinity, but reached saturation at salinity levels above 35 ppt (Fig. 4A). Exponential models were fitted to the response of foliar Na^+ concentrations as a function of salinity with R^2 values 0.53, 0.75 and 0.59 for the 280, 400 and 800 ppm CO_2 treatments, respectively. Maximal tissue Na^+ concentrations were calculated by the models to be 46.9 (±9.1 SE), 40.5 (±4.3 SE) and 40.5 mg g^{-1} (±3.8 SE) for the 280, 400 and 800 ppm CO_2 treatments, respectively. Potassium concentrations showed an opposite trend to Na^+, decreasing exponentially as salinity levels increased (Fig. 4B). Exponential models were fitted to the response of foliar K^+ concentrations as a function of salinity with R^2 values 0.52, 0.70 and 0.71 for the 280, 400 and 800 ppm CO_2 treatments, respectively. The minimum K^+ concentrations calculated by the models were 8.9 (±20 SE), 16.3 (±2.7) and 18 (±2.3) mg g^{-1} for the 280, 400 and 800 ppm CO_2 treatments. CO_2 concentrations did not affect foliar K^+ concentrations ($F_{(6,66)} = 0.94$, $P = 0.47$). Phosphorus concentrations were significantly higher in high salinity plants ($F_{(1,71)} = 18.7$, $P < 0.001$; Fig. 4C) and also significantly higher in leaves of seedlings grown under 280 ppm CO_2 ($F_{(2,71)} = 9.2$, $P < 0.001$) compared with seedlings grown at higher CO_2 concentrations.

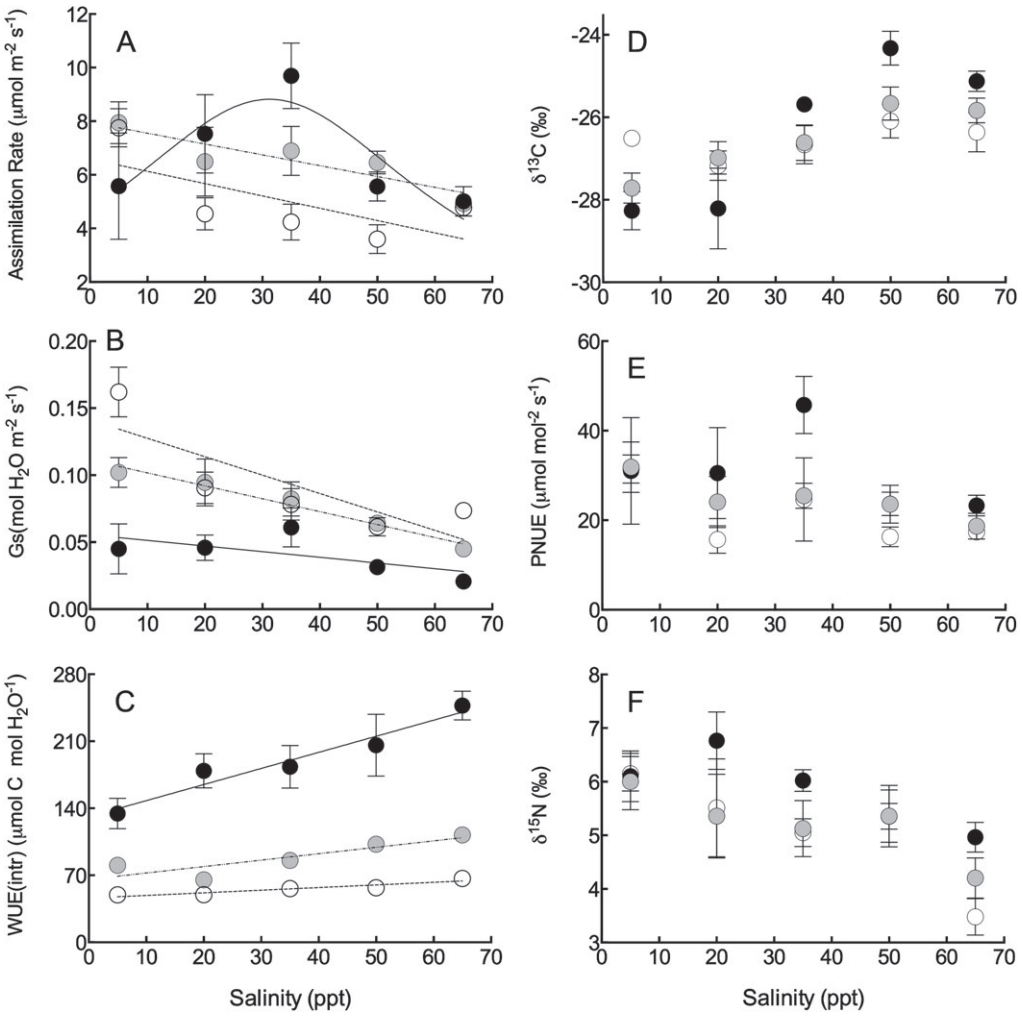

Fig. 5. Photosynthetic gas exchange values and foliar stable isotopic composition as a function of soil salinity for seedlings grown under three different atmospheric CO_2 concentrations: 280 ppm (open circles), 400 ppm (gray shaded circles) and 800 ppm (filled circles). Linear regression lines were fitted where linear relationships were significant (dotted line, 280 ppm; dashed line, 400 ppm, solid line, 800 ppm) (A) carbon assimilation rate: $A = -0.04Sal + 6.4$, $R^2 = 0.53$, and $A = -0.04Sal + 8$, $R^2 = 0.85$ for 280 and 400 ppm, respectively, for 800 ppm a Gaussian relationship is presented. (B) stomatal conductance to water vapor: $Gs = -0.0013Sal + 0.14$, $R^2 = 0.75$, $Gs = -0.0012Sal + 0.13$, $R^2 = 0.97$ and $Gs = -0.00042Sal + 0.06$, $R^2 = 0.42$ for 280, 400 and 800 ppm, respectively. (C) Intrinsic water use efficiency: $WUEi = 0.27Sal + 46.2$, $R^2 = 0.88$, $WUEi = 0.67Sal + 66$, $R^2 = 0.74$, $WUEi = 1.68Sal + 131.2$, $R^2 = 0.94$ for 280, 400 and 800 ppm, respectively. Values of (A–C) are the average of 7–10 seedlings per treatment. (D) $\delta^{13}C$ isotope ratios (E) Light saturated carbon assimilation rate per unit N_{area} (PNUE) and (F) $\delta^{15}N$ isotope ratios. Values of (D–F) are the average (±SE) of four to five seedlings per treatment.

Gas exchange

Salinity had a significant effect on mangrove seedling light saturated carbon assimilation rate (Fig. 5A). Assimilation rates were significantly reduced by salinity (ANCOVA, $F_{(1,120)} = 11.9$, $P < 0.001$; Fig. 5A) in the 280 and 400 ppm CO_2 treatments. The response of seedlings to salinity in the 800 ppm CO_2 treatment was unimodal due to the depression of photosynthetic gas exchange at both low and high salinities and was thus fitted with a Gaussian model [$A_{max} = 8.8/(1 + ((\text{salinity} - 31.2)/33.3)^2)$, $R^2 = 0.19$; Fig. 5A]. The mean distribution center (peak assimilation rate) occurred at a salinity level of 31.2 ppt (±3.8 SE). Glasshouse CO_2 concentrations also had a significant effect on assimilation rate (ANCOVA, $F_{(2,120)} = 5.17$, $P = 0.007$), with assimilation rates under preindustrial CO_2 conditions significantly lower than those under present and future concentrations (Tukey HSD, P–A, $P = 0.02$; P–F, $P = 0.02$; Fig. 5A). Assimilation rates under present and predicted future CO_2 concentrations did not significantly differ from each other (Tukey HSD, $P = 0.98$).

Stomatal conductance was significantly reduced both with increasing salinity levels and increasing CO_2 concentrations (ANCOVA, $F_{(1,120)} = 49$, $P < 0.001$ and $F_{(2,120)} = 23.3$, $P < 0.001$, respectively; Fig. 5B). At 800 ppm CO_2 treatment, stomatal conductance was significantly lower than under both 400 and 280 ppm concentrations (Tukey HSD, $P < 0.0001$ for both). Stomatal conductance was not significantly different between the 280 and 400 ppm treatment ($P = 0.1$). CO_2 concentration did not significantly alter the effect of salinity on stomatal conductance (ANCOVA, $F_{(2,118)} = 2.9$, $P = 0.06$; Fig. 5B).

Corresponding to the decrease in transpiration rates, water use efficiency (WUEi) was significantly improved as glasshouse CO_2 concentrations increased (ANCOVA, $F_{(2,118)} = 166.8$ $P < 0.0001$; Fig. 5C), more so at higher salinities ($F_{(2,118)} = 7.77$, $P < 0.001$; Fig. 5C). WUEi also significantly improved as salinity increased ($F_{(1,118)} = 48.7$, $P < 0.001$; Fig. 5C). Foliar carbon isotope ratios were significantly affected by both salinity and CO_2. $\delta^{13}C$ significantly increased as salinity levels increased ($F_{(1,65)} = 44.2$, $P < 0.001$; Fig. 5D) and was also significantly higher in the high CO_2 treatment ($F_{(2,65)} = 37.2$, $P < 0.001$; Fig. 5D), especially at higher salinities ($P < 0.001$).

Light saturated carbon assimilation rate per unit N_{area} (PNUE) significantly decreased with salinity (ANCOVA, $F_{(1,63)} = 4.8$ $P = 0.03$; Fig. 5E), and increased with CO_2 concentrations ($F_{(2,63)} = 3.46$ $P = 0.04$). PNUE was significantly lower in plants growing at 280 ppm relative to plants growing at 800 ppm (Tukey HSD, $P = 0.03$), but at 400 ppm PNUE was not significantly different from that in the 280 and 800 ppm treatments. PNUE levels were highest in plants growing in the 35 ppt treatment in the high CO_2 treatment (Fig. 5E). Stable isotope N ratios were also significantly affected by both salinity and CO_2 concentrations (Fig. 5F). $\delta^{15}N$ decreased with salinity ($F_{(1,66)} = 25$, $P < 0.001$) but increased with CO_2 concentrations ($F_{(2,66)} = 3.6$, $P = 0.03$).

Discussion

Elevated CO_2 had a significant effect on the response to salinity in the common and widespread mangrove *A. germinans*. The highest stem elongation and photosynthetic rates of seedlings grown at 800 ppm CO_2 concentrations were achieved at higher salinities than for seedlings grown under lower CO_2 concentrations. Furthermore, at low salinities, growth rates were significantly lower under future CO_2 concentrations than current and preindustrial CO_2 concentrations and mortality rates were significantly higher. Such a differential response to salinity under changing atmospheric CO_2 could influence the intensity and outcome of competitive interactions between *A. germinans* and other co-occurring species, including other mangrove species and tidal marsh vegetation. Our data suggest there may be a shift along the salinity axis of the 'fundamental niche' (Hutchinson 1957) of *A. germinans* seedlings as CO_2 concentrations in the atmosphere have increased. This could be another contributing factor to the encroachment of *Avicennia* sp. into endangered coastal saltmarsh habitats around the world over the past century (Osland et al. 2013, Saintilan et al. 2014). The change in the fundamental salinity niche due to increases in CO_2 should be taken into consideration in species distribution models that predict future distributions of salt tolerant plants under different climate change scenarios based on data collected under current or previous atmospheric CO_2 concentrations.

In addition to the shift in salinity optima for growth, a stimulation of photosynthesis and growth under elevated CO_2 occurred in plants growing in mid-range/optimal salinity (20–35 ppm). At this salinity range, carbon assimilation and stem extension rates in plants grown at 800 ppm were double those of plants growing at 280 ppm. CO_2 concentrations had a significant impact on water use efficiency as evidenced by both the increase in the foliar carbon isotopic ratio and the WUEi gas exchange calculations. Stomatal conductance declined with increases in CO_2, and at 800 ppm stomatal conductance reached values less than a third of those at 280 ppm, which is consistent with responses of most plants to elevated CO_2 (Wullschleger et al. 2002, Nowak et al. 2004, Ainsworth and Long 2005), including mangroves (Snedaker and Araújo 1998). The improved water use efficiency could explain the improved growth and productivity at mid-range salinities under high CO_2 concentrations and the shift in the salinity optima for growth.

Our data support earlier observations that elevated CO_2 stimulates growth of plants under moderately high salinity but does not lead to the alleviation of salinity stress at supraoptimal salinity conditions (Ball and Munns 1992, Ball et al. 1997, Munns et al. 1999). At 65 ppt, growth and photosynthesis were reduced under all CO_2 concentrations compared with plants grown at lower salinity levels. In mangroves of the genus *Rhizophora*, elevated CO_2 improved growth only at lower salinities (Ball et al. 1997). A study of salt marsh productivity under elevated CO_2 found growth (measured as surface elevation gain) was stimulated only at salinities lower than 10 ppt (the optimal salinity for the species) (Langley et al. 2009). This is probably due to the fact that inhibition of growth due to salinity stress is the result of a range of non-stomatal limitations, such as ion toxicity and nutrient deficiency and that CO_2 concentrations do not directly affect these processes. In

our study, Na^+ concentrations increased with increasing salinity, but reached a plateau at salinities above 35 ppt. It is possible that this is the highest Na^+ level this species can sequester in the vacuole without the leakage of Na^+ into the cytoplasm and could be the reason for declines in growth and photosynthesis above this threshold. Potassium concentrations decreased in a manner that indicated a displacement of K^+ by Na^+ at higher salinities, probably in the cell vacuole (Ball et al. 1987). CO_2 concentrations did not affect ion concentrations, which could explain why under supraoptimal salinity conditions, CO_2 did not affect mangrove productivity, growth and survivorship.

Under optimal salinity conditions, leaf SLA was lower in the high CO_2 treatment and had greater C:N ratios. This is a common phenomenon in plants growing in CO_2 enriched environments, including mangroves (Farnsworth et al. 1996), which arises in part from an increase in the rate of photosynthesis which exceeds the rate of the sink capacity to utilize the photosynthates for growth. A herbarium study on the congeneric *Avicennia marina* revealed leaf SLA of mature trees has been decreasing with increasing levels of CO_2 over the past two centuries (Reef and Lovelock 2014), suggesting that our short-term measurements of increasing rates of photosynthesis due to elevated CO_2 are likely to be maintained over longer periods. Under supraoptimal salinity conditions leaf SLA did not decrease in the high CO_2 treatment, thus it is unlikely that the inhibition of photosynthesis under high salinity conditions is due to limited sink capacity or CO_2 limitation to growth.

We detected a significant difference in root architecture in response to elevated CO_2, for example, the development of more fine roots and a decrease in SRL compared with plants grown at 400 and 280 ppm. While this is the first report for a decrease in SRL with elevated CO_2 in mangroves, a meta-analysis of nine studies of conifers and deciduous tree species also showed reductions in SRL with elevated CO_2 (Ostonen et al. 2007). Similar reductions were observed in grassland species (Anderson et al. 2010). Reduction of SLR within a species in response to elevated CO_2 could reflect enhanced nutrient absorption by the roots to increase the sink capacity for photosynthates. Our observation of higher PNUE and lower SLA (which could indicate sink limitations for photosynthates) under elevated CO_2 conditions is consistent with the hypothesis that a nutrient deficiency was developing in those seedlings. While SLR decreased with increasing CO_2, root tissue density significantly increased. Increased salinity also had a significant negative effect on SLR. Similar to the effect of elevated CO_2, the reduction in SLR corresponded to an increase in root tissue density with salinity. This could be indicative of lignification and suberization of the roots that occurs under high salinity conditions to limit the apoplastic uptake of salt into the xylem (Krishnamurthy et al. 2014).

In conclusion, atmospheric CO_2 concentrations may have significant effects on the salinity niche occupied by *A. germinans* and thus could have implications for interspecific interactions among mangrove species and between mangroves and tidal marsh vegetation in *Avicennia* dominated forests with salinities below 50 ppt, such as those of southern Australia, New Zealand (Morrisey et al. 2010), Africa and the United States. We also anticipate significant changes to water relations and nutrient cycling within the mangrove forest. It is possible that eutrophication will have a significant impact on how mangroves respond to elevated CO_2, with greater responses expected where nutrient availability is higher. However, these responses could be dependent on other factors such as interspecific competition (McKee and Rooth 2008). Increases in levels of atmospheric CO_2 may not lead to large increases in primary production, but to more subtle effects such as changes in salinity optima for growth, changes in the strength of nutrient limitations to growth and leaf and root traits that could lead to changes in species distributions and ecosystem services.

Author contributions

R. R., K. W. and C. E. L. designed the study. R. R., K. W., J. M., D. L. R. and F. M. A. conducted the study, R. R. and C. E. L. analyzed the data, R. R., K. W. and C. E. L. wrote the manuscript. Funding was secured by R. R. and K. W.

Acknowledgements – We would like to thank Dr Ken Krauss, Prof. Wayne Sousa, Dr Helene Muller-Landau and Dr Egbert Leigh for fruitful discussions and Dr Ivania Ceron, Jorge Aranda and Maya and Ethan Reef for assistance in the field. Dr Ben Turner and Dayana Agudo for mineral element and stable isotope analysis, Milton Garcia for microclimate measurements. This work has been funded by a 2012 Queensland-Smithsonian Fellowship to R. R. and by an Australian Research Council Discovery Early Career Research Award (DE120101706) to R. R. The mangrove propagules were collected under permit from ANAM, Panamá (SC/P-21-12).

References

Ainsworth EA, Long SP (2005) What have we learned from 15 years of free-air CO_2 enrichment (FACE)? A meta-analytic review of the responses of photosynthesis, canopy properties and plant production to rising CO_2. New Phytol 165: 351–372

Ainsworth EA, Rogers A, Nelson R, Long SP (2004) Testing the "source–sink" hypothesis of down-regulation of photosynthesis in elevated [CO_2] in the field with single gene substitutions in *Glycine max*. Agric For Meteorol 122: 85–94

Anderson LJ, Derner JD, Polley HW, Gordon WS, Eissenstat DM, Jackson RB (2010) Root responses along a subambient to elevated CO_2 gradient in a C3–C4 grassland. Glob Chang Biol 16: 454–468

Ball MC (1988) Ecophysiology of mangroves. Trees 2: 129–142

Ball MC (1998) Mangrove species richness in relation to salinity and waterlogging: a case study along the Adelaide River floodplain, northern Australia. Glob Ecol Biogeogr Lett 7: 71–82

Ball M (2002) Interactive effects of salinity and irradiance on growth: implications for mangrove forest structure along salinity gradients. Trees 16: 126–139

Ball MC, Munns R (1992) Plant responses to salinity under elevated atmospheric concentrations of CO_2. Aust J Bot 40: 515–525

Ball MC, Chow WS, Anderson JM (1987) Salinity-induced potassium deficiency causes loss of functional photosystem II in leaves of the grey mangrove, *Avicennia marina*, through depletion of the atrazine-binding polypeptide. Funct Plant Biol 14: 351–361

Ball MC, Cochrane MJ, Rawson HM (1997) Growth and water use of the mangroves *Rhizophora apiculata* and *R. stylosa* in response to salinity and humidity under ambient and elevated concentrations of atmospheric CO_2. Plant Cell Environ 20: 1158–1166

Bunt J, Williams W, Clay H (1982) River water salinity and the distribution of mangrove species along several rivers in North Queensland. Aust J Bot 30: 401–412

Cernusak LA, Winter K, Martínez C, Correa E, Aranda J, Garcia M, Jaramillo C, Turner BL (2011) Responses of legume versus nonlegume tropical tree seedlings to elevated CO_2 concentration. Plant Physiol 157: 372–385

Drake BG, Gonzàlez-Meler MA, Long SP (1997) more efficient plants: a consequence of rising atmospheric CO_2? Annu Rev Plant Physiol Plant Mol Biol 48: 609–639

Farnsworth EJ, Ellison AM, Gong WK (1996) Elevated CO_2 alters anatomy, physiology, growth, and reproduction of red mangrove (*Rhizophora mangle* L.). Oecologia 108: 599–609

Geissler N, Hussin S, Koyro H-W (2009) Elevated atmospheric CO_2 concentration ameliorates effects of NaCl salinity on photosynthesis and leaf structure of *Aster tripolium* L. J Exp Bot 60: 137–151

Goncalves-Alvim SJ, Santos MCFV, Fernandes GW (2001) Leaf gall abundance on *Avicennia germinans* (Avicenniaceae) along an interstitial salinity gradient. Biotropica 33: 69–77

Hutchings P, Saenger P (1987) Ecology of Mangroves. University of Queensland Press, St Lucia

Hutchinson GE (1957) Concluding remarks. Cold Spring Harb Symp Quant Biol 22: 415–427

Krishnamurthy P, Jyothi-Prakash PA, Qin LIN, He JIE, Lin Q, Loh C-S, Kumar PP (2014) Role of root hydrophobic barriers in salt exclusion of a mangrove plant *Avicennia officinalis*. Plant Cell Environ 37: 1656–1671

Langley JA, McKee KL, Cahoon DR, Cherry JA, Megonigal JP (2009) Elevated CO_2 stimulates marsh elevation gain, counterbalancing sea-level rise. Proc Natl Acad Sci USA 106: 6182–6186

Lin G, Sternberg L (1992) Effect of growth form, salinity, nutrient and sulfide on photosynthesis, carbon isotope discrimination and growth of red mangrove (*Rhizophora mangle* L.). Funct Plant Biol 19: 509–517

Lovelock CE, Ball MC, Feller IC, Engelbrecht BMJ, Ewe ML (2006) Variation in hydraulic conductivity of mangroves: influence of species, salinity, and nitrogen and phosphorus availability. Physiol Plant 127: 457–464

Lugo AE, Snedaker SC (1974) The ecology of mangroves. Annu Rev Ecol Syst 5: 39–64

McKee KL, Rooth JE (2008) Where temperate meets tropical: multi-factorial effects of elevated CO_2, nitrogen enrichment, and competition on a mangrove-salt marsh community. Glob Chang Biol 14: 971–984

Morrisey DJ, Swales A, Dittmann S, Morrison MA, Lovelock CE, Beard CM (2010) The ecology and management of temperate mangroves. In: Gibson RN, Atkinson RJA, Gordon JDM (eds) Oceanography and Marine Biology: An Annual Review. CRC Press, Boca Raton, pp 43–160

Munns R, Cramer GR, Ball MC (1999) Interactions between rising CO_2, soil salinity and plant growth. In: Luo Y, Mooney HA (eds) Carbon Dioxide and Environmental Stress. Academic Press, San Diego, pp 139–167

Nowak RS, Ellsworth DS, Smith SD (2004) Functional responses of plants to elevated atmospheric CO_2 – do photosynthetic and productivity data from FACE experiments support early predictions? New Phytol 162: 253–280

Odum WE, McIvor CC, Smith TJ (1982) The Ecology of the Mangroves of South Florida: A Community Profile. United States Fish and Wildlife Service, Office of Biological Services, Washington, DC

Osland MJ, Enwright N, Day RH, Doyle TW (2013) Winter climate change and coastal wetland foundation species: salt marshes vs. mangrove forests in the southeastern United States. Glob Chang Biol 19: 1482–1494

Ostonen I, Püttsepp Ü, Biel C, Alberton O, Bakker MR, Lõhmus K, Majdi H, Metcalfe D, Olsthoorn AFM, Pronk A, Vanguelova E, Weih M, Brunner I (2007) Specific root length as an indicator of environmental change. Plant Biosyst 141: 426–442

Pritchard SG, Peterson CM, Prior SA, Rogers HH (1997) Elevated atmospheric CO_2 differentially affects needle chloroplast ultrastructure and phloem anatomy in *Pinus palustris*: interactions with soil resource availability. Plant Cell Environ 20: 461–471

Reef R, Lovelock CE (2014) Historical analysis of mangrove leaf traits throughout the 19th and 20th centuries reveals differential responses to increases in atmospheric CO_2. Glob Ecol Biogeogr 23: 1209–1214

Saintilan N, Wilson NC, Rogers K, Rajkaran A, Krauss KW (2014) Mangrove expansion and salt marsh decline at mangrove poleward limits. Glob Chang Biol 20: 147–157

Scholander PF, Hammel HT, Hemmingsen E, Garey W (1962) Salt balance in mangroves. Plant Physiol 37: 722–729

Smith TJ (1988) Differential distribution between subspecies of the mangrove *Ceriops tagal*: competitive interactions along a salinity gradient. Aquat Bot 32: 79–89

Snedaker SC, Araújo RJ (1998) Stomatal conductance and gas exchange in four species of Caribbean mangroves exposed to ambient and increased CO_2. Mar Freshw Res 49: 325–327

Stitt M, Krapp A (1999) The interaction between elevated carbon dioxide and nitrogen nutrition: the physiological and molecular background. Plant Cell Environ 22: 583–621

Thomas RB, Strain BR (1991) Root restriction as a factor in photosynthetic acclimation of cotton seedlings grown in elevated carbon dioxide. Plant Physiol 96: 627–634

Wullschleger SD, Tschaplinski TJ, Norby RJ (2002) Plant water relations at elevated CO_2 – implications for water-limited environments. Plant Cell Environ 25: 319–331

Supporting Information

Additional Supporting Information may be found in the online version of this article:

Fig. S1. Representative light curves of three seedlings grown at different salinity and CO_2 conditions. For each leaf, assimilation rate was measured for nine light levels (2000, 1500, 1000, 500, 200, 100, 50, 20 and 0 μmol). Data were fitted with the Mitscherlich model equation ($R^2 \geq 0.98$ for all three curves). The light saturated rate of photosynthesis was achieved at irradiances of <600 μmol.

Fig. S2. The relationship between SL and leaf number in *Avicennia germinans* seedlings grown under three CO_2 concentrations: 280 ppm (open circles), 400 ppm (gray filled circles) and 800 ppm (black filled circles). Data were fitted with linear models: 280 ppm (broken line), leaf $\# = 0.38SL + 2.7$, $R^2 = 0.41$; 400 ppm (solid gray line) leaf $\# = 0.46SL + 0.7$, $R^2 = 0.48$; 800 ppm (solid black line) leaf $\# = 0.58SL - 0.9$, $R^2 = 0.7$. Slopes were not significantly different among the three treatments ($P = 0.14$)

Edited by J. Marshall